LA-UR-74-1883

CONF-741105--50

TITLE: CARBON DIOXIDE LASER DEVELOPMENT AND ASYMMETRY IN LASER DRIVEN IMPLOSIONS

AUTHOR(S): R. F. Benjamin, Keith Boyer, E. H. Farnum, C. A. Fenstermacher, R. J. Fries, D. V. Giovanielli, R. P. Godwin, A. J. Lieber, G. H. McCall, and T. F. Stratton

SUBMITTED TO: Publications section, International Atomic Energy Agency, Vienna, Austria

(Talk given at the 5th Conference on Plasma Physics and Control Nuclear Fusion Research Tokyo, Japan, November 11 thru 15, 1974.)

LASL-AEC-OFFICIAL

MASTER

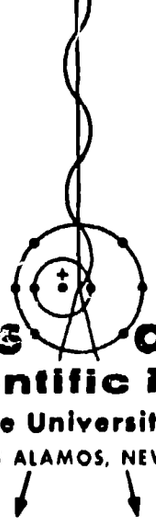

los alamos
scientific laboratory
of the University of California
LOS ALAMOS, NEW MEXICO 87544

LASL-AEC-OFFICIAL

Form No. 836
St. No. 2629
1/73

UNITED STATES
ATOMIC ENERGY COMMISSION
CONTRACT W-7405-ENG. 36

CARBON DIOXIDE LASER DEVELOPMENT AND ASYMMETRY IN LASER DRIVEN IMPLOSIONS*

R. F. Benjamin, Keith Boyer, E. H. Farnum, C. A. Fenstermacher,
R. J. Fries, D. V. Giovanielli, R. P. Godwin,
A. J. Lieber, G. H. McCall, and T. F. Stratton

Los Alamos Scientific Laboratory
University of California
Los Alamos, New Mexico 87544

Introduction

Experimental investigations of the interaction of very intense light beams with plasma at high density are necessary to confirm theoretical concepts for laser-induced fusion. The fundamental requirements for such fusion are set forth in papers by Kidder and Boyer.[1,5] Theoretical analyses of the process indicate requirements for laser pulse energy greater than 10 kJ delivered in pulses shorter than 1 ns[2] The overall laser efficiency should be as great as possible and for commercial applications should be greater than 10%. Three laser systems are known which can reach these energies and power levels: Nd:glass,[3] atomic iodine,[4] and CO_2.[5] Only the electrically-excited CO_2 laser, however, shows reasonable promise of achieving an overall efficiency approaching 10% for short pulses.

The successful production of extremely intense pulses of CO_2 laser energy depends on the development of an oscillator-amplifier system that operates at gas pressures sufficiently great to provide adequate bandwidth and economical energy storage, that is, at supra-atmospheric pressures. The LASL laser system consists of an oscillator and 4 amplifier stages, all operating at atmospheric pressure or above. A schematic drawing of the laser system and typical operating parameters are shown in Fig. 1. The oscillator is a conventional TEA laser,[6] actively mode-locked, which generates single frequency (P-20) TM_{00} pulses of 1.2 ns width. The amplifiers are all externally ionized (e-beam) lasers of Los Alamos design.[7] The mode-locked pulse is first amplified by 2 m of preamplifier stages at 1 atmosphere pressure operating essentially in the small signal region and then by 3 m

LASL-AEC-OFFICIAL

*Work performed under the auspices of the U. S. Atomic Energy Commission.

of heavily saturated power amplifiers at > 2 atmospheres pressure. The single-pass small-signal gain through the system is in excess of 10^9. Operating in saturation with interstage isolators, the pulse power gain is about 10^6.

LASER SYSTEM DESIGN AND PERFORMANCE

Oscillator

The oscillator laser and pulse selection system produce single line Gaussian pulses in space and time which are 1.2 ns FWHM and contain about 1 mJ energy per pulse.[8] The pulse selection system, an electro-optics shutter consisting of a gallium arsenide crystal and a ten plate germanium polarizer-analyzer stack results in a pulse contrast ratio greater than 10^4:1. Work is now in progress to enlarge the options available for oscillator pulses. These options include shorter pulses, which are generated by passive and active mode-locking techniques in high pressure CO_2,[9] and oscillator pulses which contain approximately equal quantities of energy in transitions from both the 10 μm and the 9 μm vibrational bands. The need and performance of such multi-frequency operation has been described and analyzed.[10]

Amplifiers

CO_2 amplifiers at Los Alamos are based on the generation of controlled discharges in suitable gas mixtures through the application of external electron beams as the ionizing agent with electrical excitation of the lasing molecules provided by a second, nonsustaining discharge.[11] The parameters and scaling laws of these discharges and the associated molecular function have been extensively studied at LASL and are presently well understood. Problems of gas electrical breakdown and arc formation are thereby avoided and the molecular pumping efficiency can be optimized. Relatively large volumes can be uniformly ionized by the electron beam (25 x 25 x 200 cm presently) and the process can be scaled to different geometries and pressures. The amplifier chain was designed as a prototype system in which engineering and physics problems relating to the characterization and operation of larger systems could be evaluated and from which good quality laser pulses of varying energy are available for interaction experiments.

The final power amplifier of the system has active volume 2 m long, with an optical aperture of 400 cm^2, and operates at 2 atmospheric pressure. The peak inversion energy density in this amplifier is 12 joules per liter. Approximately 30% of this energy (300 joules in the optical aperture) is available on the 1.5 ns time scale of the single frequency oscillator pulse. The electrical energy deposited in the amplifier up until the moment of gain maximum is 20 kJ, for an overall electrical-to-optical efficiency (excluding heater power to the hot cathode electron gun) of 1.5%. On a unit volume basis the electrical-to-optical efficiency is 2.2%. The electrical parameters of the electron guns and the gas discharge characteristics of the four amplifiers in the chain are summarized in Fig. 2.

A particularly important question in any evaluation of CO_2 amplifiers is the efficiency of amplification of short pulses.[12,13] The population inversion energy is distributed over a rotational energy manifold of the excited vibrational level. The time scale for energy extraction from all of these rotational

sublevels by a single rotational transition requires cross-relaxation between these levels. This cross-relaxation time for energy extraction is greater than the relaxation time of a single level by the factor $1/k(J, T_r)$, ($\approx$15 for the case of interest). This factor arises because one is asking for all the energy of these levels to be extracted through the single lasing level as opposed to asking that a single level be repopulated to its equilibrium value by its fifteen neighboring levels. Hence, the total rotation reservoir is accessible only to single-line oscillator pulses with $\tau_{pulse} > \tau_{rot}/\kappa$. This limitation can be overcome provided the oscillator pulse contains frequencies corresponding to several rotational transitions for a given vibrational transition, i.e., (001→100), or alternatively it contains frequencies for the two vibrational bands (001→020 as well as 001→100) with differeing J values.[14]

Interstage and Backscatter Isolation

The suppression of interstage oscillations at high overall gain ($\sim 10^8$) has been achieved by the insertion of gas cells containing bleachable molecular gases (sulfur hexafluoride, ammonia or butane) and helium between the various amplifiers as well as through separation. The amount of bleachable absorber required to prevent prelasing is determined by measurement. This bleachable cell improves the contrast ratio of the pulse as well.

The plasma generated by the interaction of the focused laser beam with solid matter reflects as much as 5% of the incident energy back into the focusing optics of the laser system.[15] The reflection is amplified as it passes back through the amplifiers and may exceed the damage threshold of some optical components. Amplifier reflections have been eliminated by deliberately providing beam waists in the optical path where plasmas are generated at the appropriate time. When the energy density of the outgoing pulse exceeds about 4×10^8 watt/cm^2 (if it does not, a secondary laser focused on the intersection of the beam and the film is necessary) an ionized seed plasma is created which terminates the return pulse. About 20% of the outgoing pulse energy is sacrificed to generate the film plasma.

ASYMMETRY IN LASER DRIVEN IMPLOSION

The use of hollow shells as laser imploded targets results in a considerable relaxation of laser parameters. The power densities at the surface of a shell, because of the larger radius, can be lower and can, perhaps, be set below the threshold of nonlinear processes. The pulsewidth can be longer since the required pulsewidth is the time for a shock wave to propagate from the surface to the center of the target. Because the use of shells produces severe problems in asymmetries which develop as a result of the Rayleigh-Taylor instability, a study has been done at Los Alamos, using the Los Alamos ball-and-disc target shown in Fig. 3, to study the effects of asymmetries in laser beam irradiation. The ball-and-disc uses the electron thermal conduction in the plasma generated by the disc surrounding the glass microballoon to conduct energy to the rear of the microballoon when the target is heated by a single laser beam.

The intensity of the pulse used to irradiate these targets is a function of time as shown in Fig. 4. A pre-pulse having an amplitude of approximately ten percent of the main pulse was applied to the target 50 to 300 ps before the peak of the main pulse to ionize the disc and provide the conduction path. The width of the main pulse was approximately 50 ps.

A calculation of the type of behavior one might expect from such a target is shown in Fig. 5. The curve on the left indicates plasma conditions just at the end of the pre-pulse and the curve on the right indicates conditions at approximately the peak of the main pulse. One sees that a compression of approximately 100 could be generated in the shell material in a radius of about 2 to 3 μm.

The experimental apparatus used to study this effect is shown in Fig. 6, where the image-intensified x-ray pinhole camera can be seen behind the target holder. The results of two such experiments as photographed by the x-ray pinhole camera are shown in Fig. 7. The upper photograph, an isodensity trace, was produced when a pre-pulse having an amplitude of over half that of the main pulse was applied. The pre-pulse destroyed the target, and the main pulse then heated it uniformly giving the bright uniform ellipsoid shown in the photograph. In the lower photograph the proper pre-pulse amplitude and spacing were used and one can see in the bottom left photograph a bright spot appearing at the center of the target indicating that the target did collapse to a single point. An isodensity trace of this photograph (Fig. 8), however, shows that the central maximum is not completely circular but instead is almost elliptically shaped, indicating that the implosion did occur somewhat asymmetrically. The ablation region shown in the first ring around the target shows a definite scalloped structure. The efficiency of the ball-and-disc structure in heating the rear surface of the target can be seen in some pinhole photographs in which the bright region is at the rear of the target. The shell structure of the target is also quite apparent in some cases. This type of photograph results from a shot in which the spacing between the pre-pulse and main pulse was too short. A shot of this type can be seen in Fig. 9, which is a densitometer trace taken normal to the disc behind the target along the direction of the laser beam. The shell structure can be seen here. A decrease in the interior volume of a factor of 50 to 100 can also be seen, although it should be noticed that there is a difference between the front and back sections of the densitometer trace.

In summary, it appears that although some compression may have been observed in these experiments, there is evidence of asymmetries. The source of the asymmetry, whether from the Rayleigh-Taylor instability or from asymmetric heating of the target has not yet been determined.

REFERENCES

[1] KIDDER, R. E., Nuclear Fusion 8 (1968) 3.

[2] CLARK, J. S. FISHER, H. N., and MASON, R. J., Phys. Rev. Letts. 30, (1973) 89; 30, (1973) 249.

NUCKOLS, J., WOOD, L., THIESSEN, A., and ZIMMERMAN, G., Nature, (Lond.) 239, (1972) 139.

[3] BASOV, N. G., KROKHIN, O. N., and SKLIZKOV, G. V., "Laser Interaction and Related Phenomena," H. Schwartz and H. Hora, Ed., Plenum Press, NY (1972) 389.

[4] HOHLA, K., GENSEL, P., and KOMPA, K. L., ibid, p. 61.

[5] BOYER, Keith, Astronautics & Aeronautics 11 (August 1973) 44.

LASL-AEC-OFFICIAL

[6] LAMBERTON, H., and PEARSON, P., Electron Lett. 7 (1971) 141.

[7] STRATTON, T. F. ET AL., J. Quant. Elec. 9 (1973) 157.

[8] FIGUEIRA, J. F., REICHELT, W. H., and SINGER, S., Rev. Sci. Instr. 10 (1973) 1481.

[9] FELDMAN, B. J. and FIGUEIRA, J. F., Appl. Phys. Lett. 25 (1974) 301.

[10] FIGUEIRA, J. F. and SUTPHIN, H. D., submitted to Appl. Phys. Lett. (1974).

[11] FENSTERMACHER, C. A. ET AL., Appl. Phys. Lett. 20 (1972) 56.

[12] SCHAPPERT, G. T., Appl. Phys. Lett. 23 (1973) 319.

[13] STARK, E. E. ET AL., Appl. Phys. Lett. 23 (1973) 322.

[14] FELDMAN, B. J., J. Quant. Elec. 9 (1973) 1070.

[15] MITCHELL, K. B. and STRATTON, T. F., Bull. Am. Phys. Soc. 18 (1973) 1255.

LASL-AEC-OFFICIAL

FIGURE CAPTIONS

Fig. 1. Schematic of CO_2 oscillator-amplifier chain which produces pulses containing 200 J in 1.5 ns.

Fig. 2. Electrical parameters of the electron-beam controlled amplifiers.

Fig. 3. Los Alamos ball-and-disk target for producing implosion with single-beam illumination.

Fig. 4. Laser pulse used in implosion experiments.

Fig. 5. Calculated implosion target behavior. (Left) Target conditions after prepulse. (Right) Target conditions at peak of main pulse.

Fig. 6. Experimental apparatus for implosion experiments. Intensified x-ray camera is at rear.

Fig. 7. X-ray pinhole photographs of implosion experiments.

Fig. 8. Isodensity trace of an x-ray pinhole photograph showing some target asymmetry.

Fig. 9. Densitometer trace of pinhole photograph showing compression.

LASL-AEC-OFFICIAL

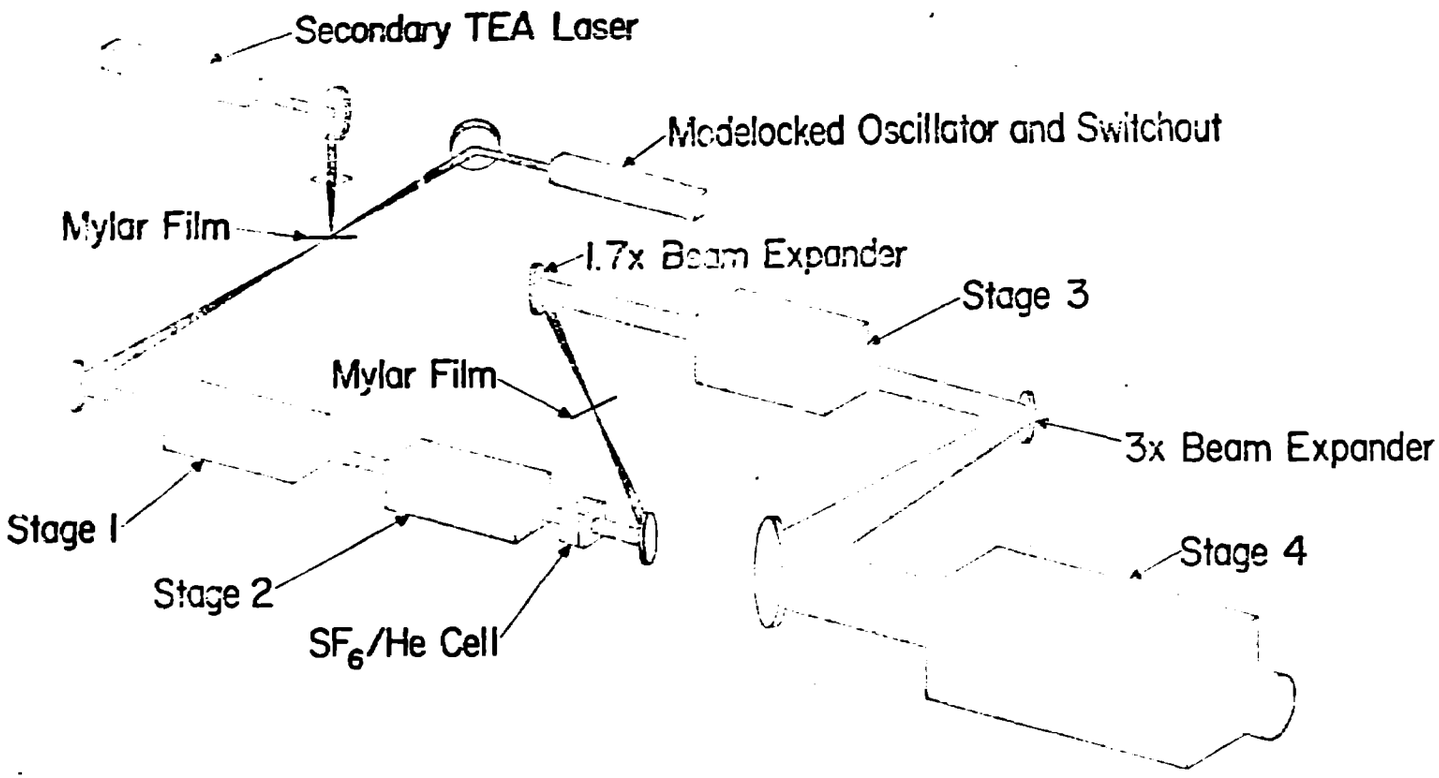

Small Signal Gain –P(20) 10^9

Saturated Gain –P(20) 2×10^5

Component	Volume Litre	Gain $e^{g_0 L}$ –P(20)	Pressure Torr	$\Delta N \hbar\omega$ Joules	Energy Out Joules	Fraction
Oscillator		5	600		<0.001	
Stage 1	1.4	165	600	12	0.1	<0.01
Stage 2	1.4	165	600	12	1.1	0.09
Stage 3	4	125	1800	100	20	0.20
Stage 4	80	320	1400	900	200	0.22

Figure 1

LASL-AEC-OFFICIAL

Parameter	Stages 1&2	Stage 3	Stage 4
Electron Beam			
Energy	120 kV	155 kV	250 kV
Current	100 A	500 A	1500 A
Current density	0.12 A/cm^2	0.60 A/cm^2	0.27 A/cm^2
Gas			
Pressure	600 torr	1800 torr	1400 torr
Electric field	4.3 kV/cm-atm	3.8 kV/cm-atm	3.5 kV/cm-atm
Current	5000 A	16000 A	50000 A
Current density	6.3 A/cm^2	20 A/cm^2	9 A/cm^2
Gain (P(20))	0.051 cm^{-1}	0.049 cm^{-1}	0.031 cm^{-1}
J/liter - atm.	150	150	85
Efficiency $\frac{g_0(J)E_s}{J/\text{liter}}$	6.5 %	6.2 %	6.9 %

los alamos
scientific laboratory
of the University of California

Figure 2

LASL-AEC-OFFICIAL

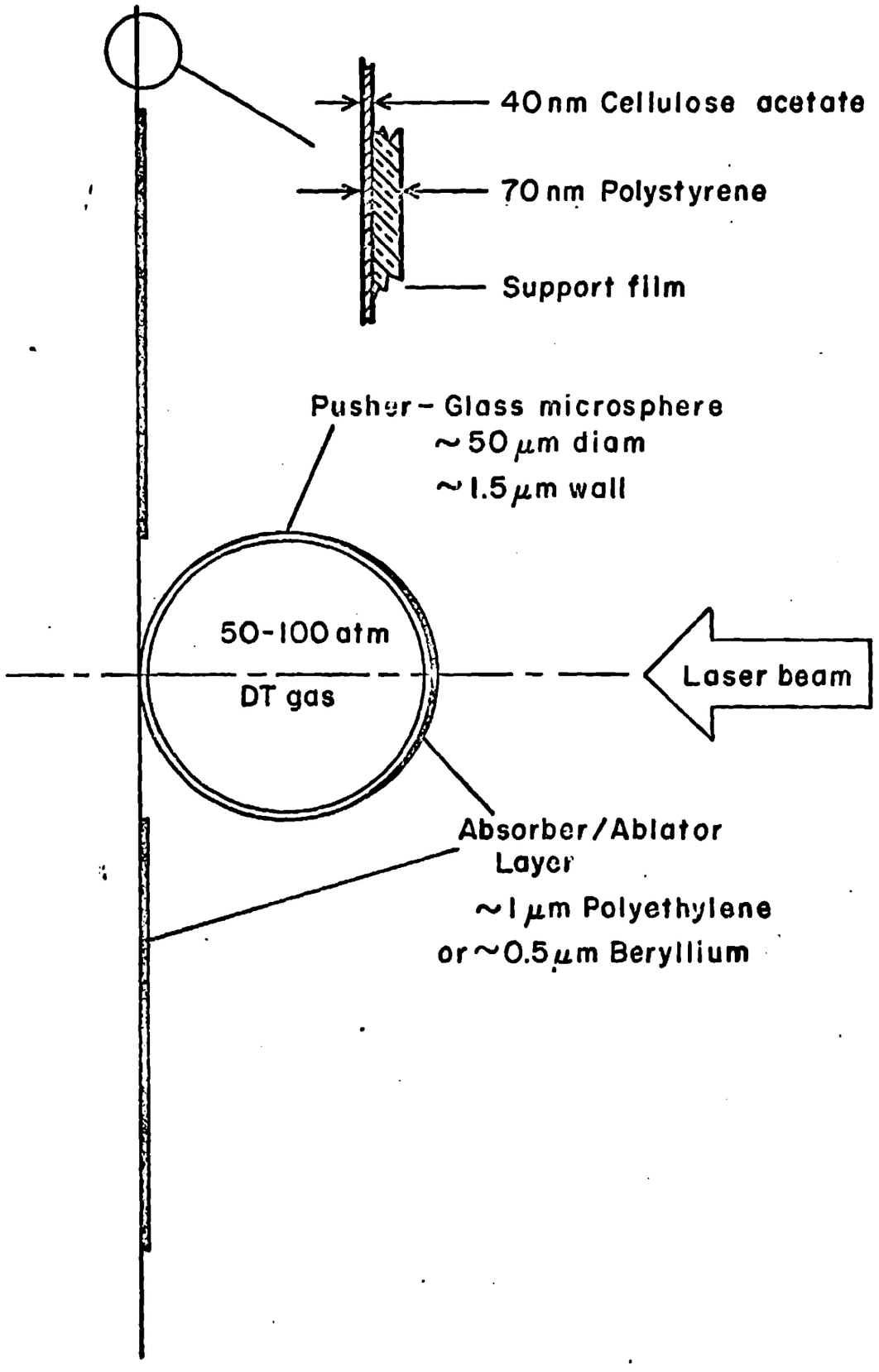

Figure 3

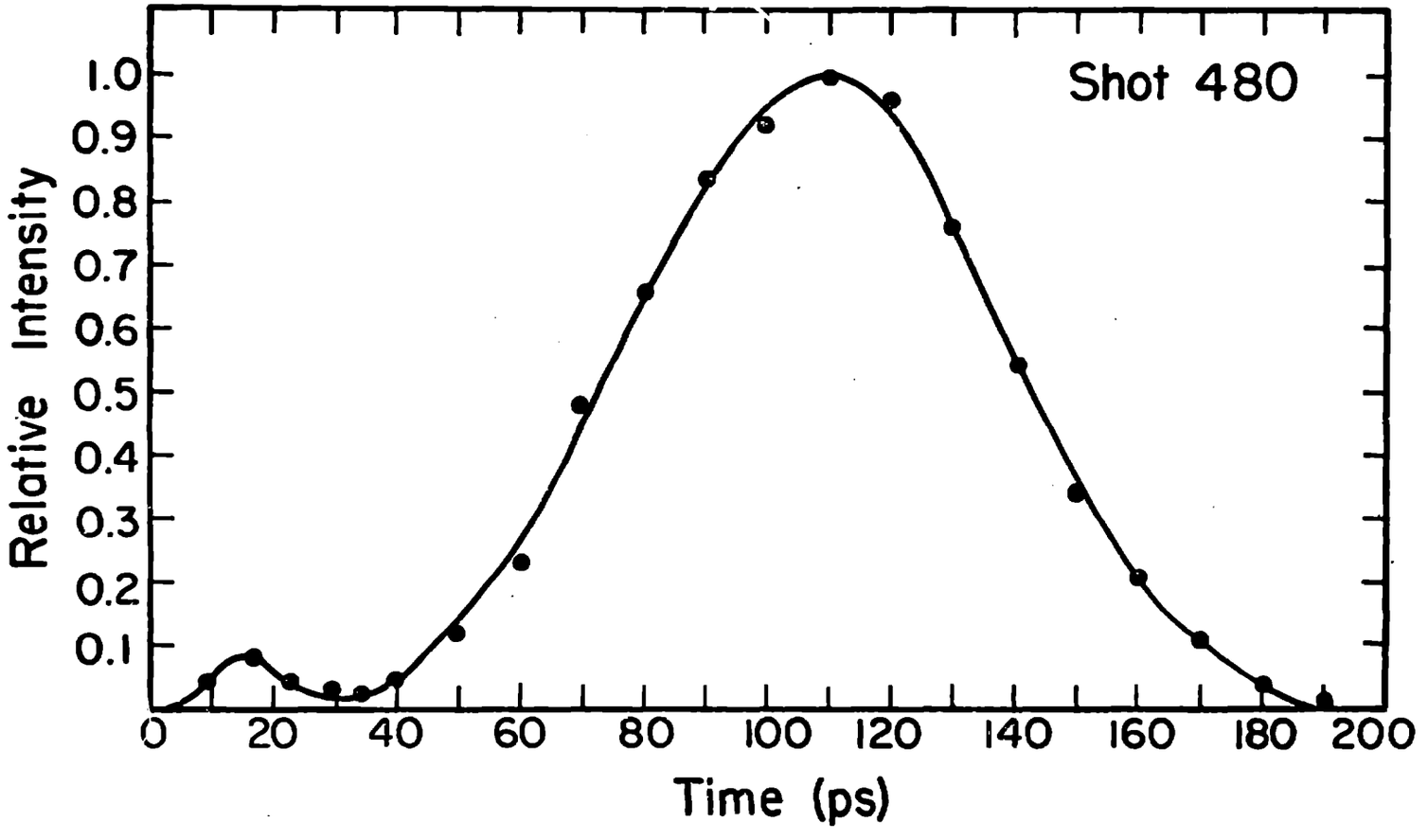

Figure 4

LASL-AEC-OFFICIAL

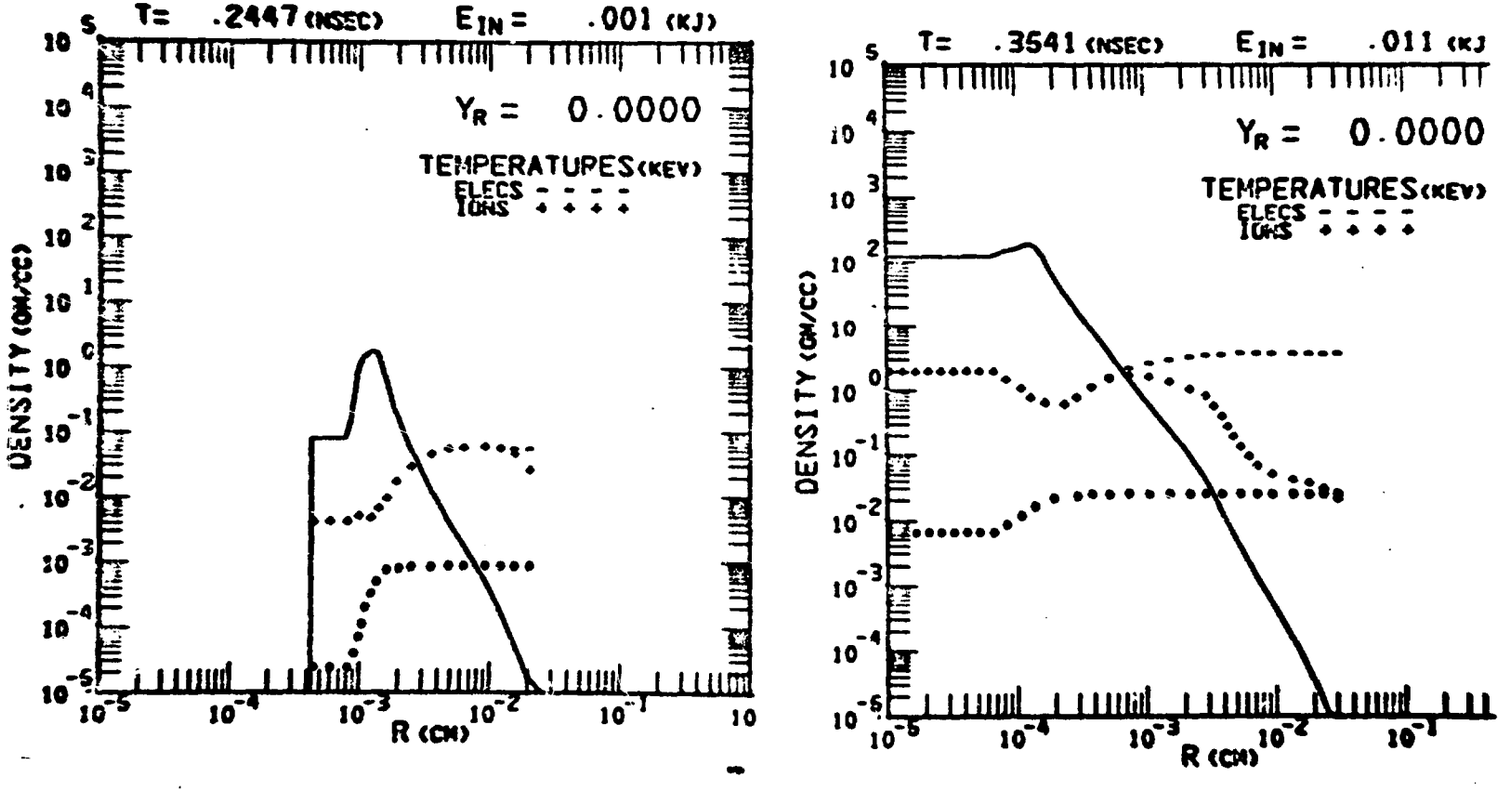

Figure 5

LASL-AEC-OFFICIAL

Figure 6

LASL-AEC-OFFICIAL

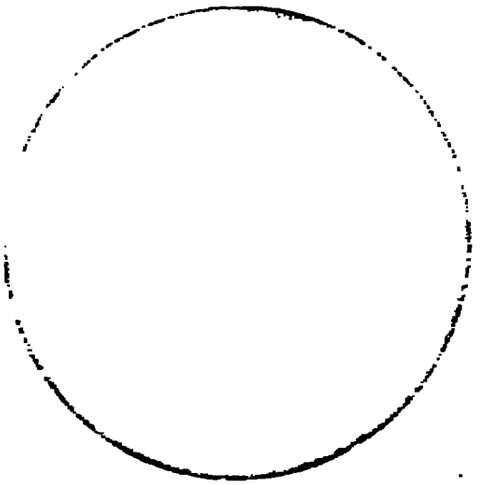

(a)

(b)

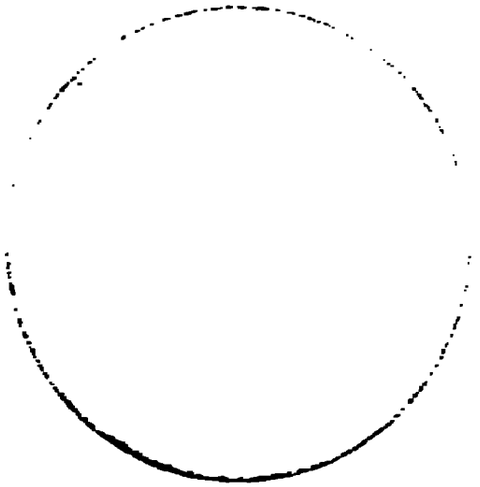

(c)

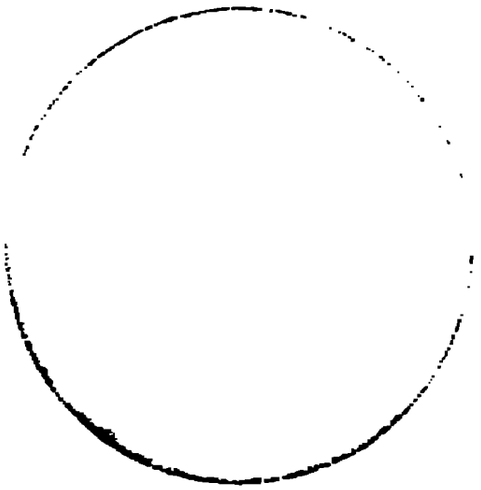

(d)

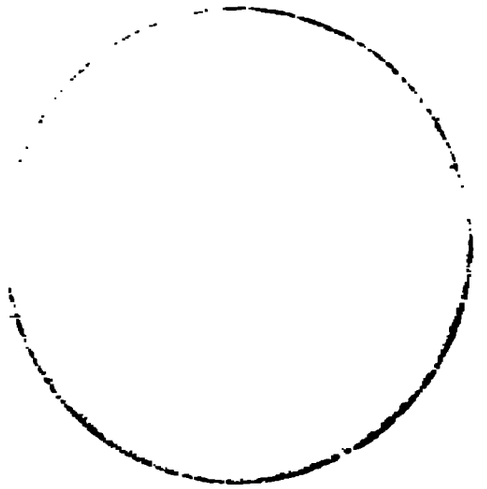

(e)

Figure 7

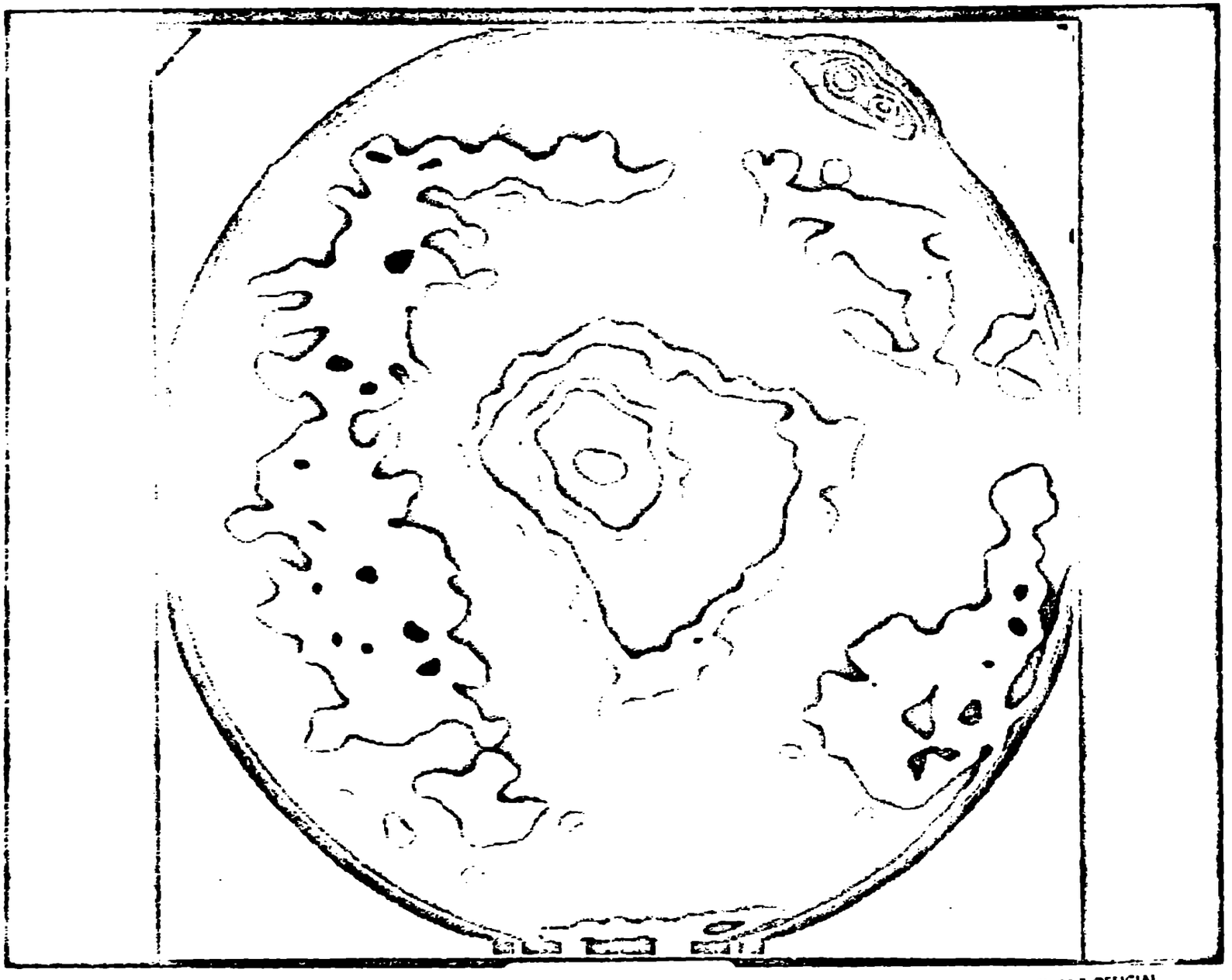

LASL-AEC-OFFICIAL

Figure 8

LASL-AEC-OFFICIAL

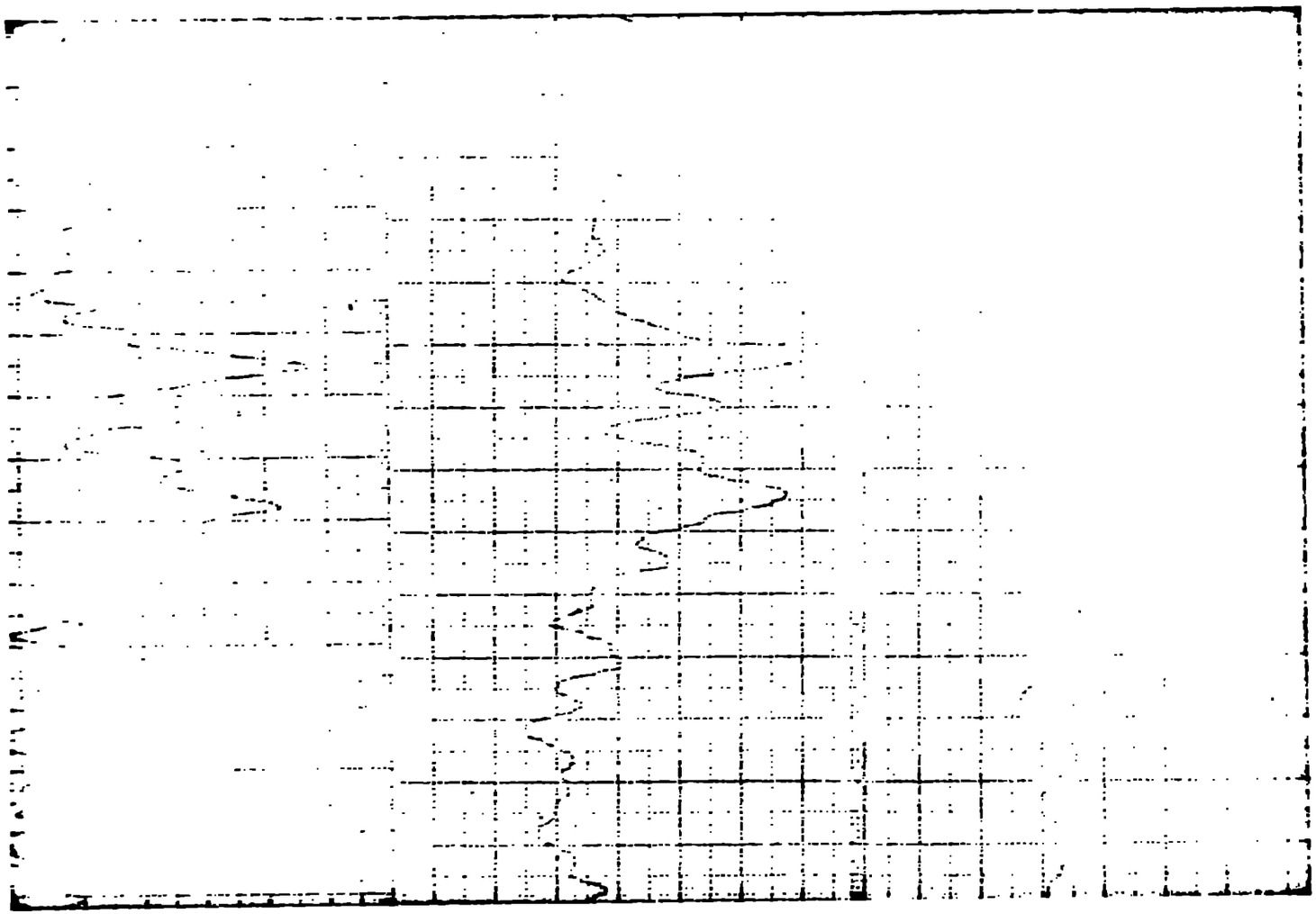

LASL-AEC-OFFICIAL